Microbial adaptation in vertical soil profiles contaminated by antimony smelting plant

Rui Xu
Guangdong Institute of Eco-environmental Science & Technology
Xiaoxu Sun
Guangdong Polytechnic of Science and Technology
Feng Han
Universite de Carthage Institut Superieur des Sciences et Technologies de l'Environnement de Borj Cedria
Enzong Xiao
Guangzhou University
Baoqin Li
Guangdong Institute of Eco-environmental Science & Technology
Lang Qiu
Guangdong Institute of Eco-environmental Science & Technology
Benru Song
Guangdong Institute of Eco-environmental Science & Technology
Zhaohui Yang
Hunan University
Weimin Sun (swmmicrobe@163.com)
Guangdong Institute of Eco-Environmental and Soil Sciences https://orcid.org/0000-0002-3456-8177

Research

Keywords: metagenomic sequencing, amplicon sequencing, soil depth, microbial interaction, soil profiles, microbial diversity

Posted Date: June 18th, 2020

DOI: https://doi.org/10.21203/rs.3.rs-34437/v1

Version of Record: A version of this preprint was published at FEMS Microbiology Ecology on September 23rd, 2020. See the published version at https://doi.org/10.1093/femsec/fiaa188.

Abstract

Background

Soil microbes play critical roles in the biogeochemical cycling of antimony (Sb) and arsenic (As), and the effects of Sb and As contamination on soil microbiota have been well documented in surface soils (< 0.2 m). However, their effects in deep soils remain poorly understood. This study determined the depth-resolved effects of Sb and As contamination on the microbial adaptation throughout soil profiles (0–2 m) and compared contaminated soil samples to uncontaminated samples.

Methods

16S rRNA amplicon sequencing and shotgun metagenomic sequencing were employed to investigate the microbial community and their metabolism traits in soil profiles. Co-occurrence network analysis was used to present the pairwise interactions of microbes.

Results

As soil depth increased, Acidobacteria (18.8%–44.7% from top to bottom, hereafter), Chloroflexi (8.7%–42.4%), Proteobacteria (11.4%–27.1%), and Thaumarchaeota (0.49%–20.17%) were the most variable phyla from surface to deep soil. A set of co-occurrence networks revealed an obvious changing pattern of microbial interactions as soil depth increased. The networks were loosely connected in the heavily contaminated surface soil but gradually recovered and were well connected in the less contaminated deep soil. Results suggested that individual species became more connected with other patterns to perform syntrophic functions in the less contaminated soil depth. Shotgun metagenomic sequencing results indicated that microbial metabolic potential also changed with soil depth. Genes encoding C metabolism pathways were negatively correlated with Sb and As concentrations. A set of arsenic-related genes was enriched by the high Sb and As contamination but reduced with soil depth.

Conclusions

Soil depth-resolved characteristics are often many meters deep and their microbial diversity and community structures obviously change along their vertical soil profiles due to different nutrient contents and biomasses. The significance of this study is that it further reveals how the microbial communities and microbial physiological traits respond to different soil profiles contaminated by high concentrations of Sb and As.

Background

Antimony (Sb) is a toxic element widely distributed in the lithosphere that mainly associates with arsenic (As) as sulfide or oxide. Sb and As are nitrogen-group elements with similar valence electron configurations and chemical speciation. Therefore, the behavior and toxicity of Sb in the environment is assumed to be similar to As. Compared to the extensively researched biogeochemistry of As, Sb is poorly

studied despite its emergence as an important contaminant [1]. Sb and As can be introduced through natural processes, such as rock weathering and volcanic activity [2]. The natural abundance of Sb and As in the soil and sediment is low [3]. However, elevated soil concentrations of Sb and As are found near Sb and As mines, in areas contaminated by human activities, and at shooting ranges, as mining and smelting processes are the leading sources of Sb and As soil pollution [4].

Generally, the concentrations of Sb and As in contaminated soils accumulate in surface soils (by tensive effects) and gradually decline in deeper layers (by fewer effects) due to atmospheric deposition [5], which lead to different environmental risks at different soil depths. Additionally, various geochemical factors, such as oxidation-reduction potential (Eh), pH, and organic matter, may vary along the vertical soil profile, which further lead to changes in the distribution, migration, speciation, and toxicity of Sb and As at different soil depths [6]. Therefore, the behavior of Sb and As in the environment, including their total contents, oxidation states, bonding-forms, and sorption characteristics, are largely affected by soil depth.

Soil microbiota are critical factors that affect the behavior of Sb and As by altering their soil properties or directly affecting Sb and As [5]. It has been demonstrated that microorganisms mediate the biogeochemical cycling of Sb and As by detoxification, precipitation, and mobilization [7-9]. Sb and As contamination released to surface soil during smelting activities inevitably affects the microbial communities and their ecological functions in deep soil layers. However, our understanding of the structure diversity and metabolic traits of soil microbial communities in Sb- and As-contaminated areas is limited to surface soils, as the vast majority of studies focus solely on the top 15 cm of the soil column where the microbial biomass is the greatest [1, 10, 11]. As a result, the effects of Sb and As contamination on soil microbiota in deeper soil depths have not been well characterized and the spatial variability exhibited by these communities remains poorly understood. In particular, soil depth-resolved profiles are often many meters deep and their microbial diversity and community structures obviously change along their vertical soil profiles due to different nutrient contents and biomasses [10]. Thus, deeper soil layers may contain microbial communities that are specialized to their environment and fundamentally distinct from surface communities [10, 12]. Based on these findings, we hypothesize that the changes in microbial communities in deeper soil layers are determined by smelting contamination, which will differ from surface soil that is affected by direct contamination. Therefore, the behavior of Sb and As contamination and soil microbiota will change throughout soil profile depths, which may in turn affect their correlation with contaminant transformation or ecosystem biogeochemistry.

To test these hypotheses, two soil profiles (as duplicates) that were severely affected by smelting activities were selected and compared to one uncontaminated profile. Samples were collected from surface soil and deep soil layers (ranging from 0–2 m) for geochemical measurement, 16S rRNA amplicon sequencing analysis, and shotgun metagenomic sequencing analysis. We expected the strong geochemical gradients found within the soil profiles to cause changes in their microbial community compositions and metabolic traits as well as further reveal microbial adaptations to smelting contamination in different profile depths.

Methods

Collection of soil samples

Research area located at the Yanshan Sb mine smelter, Lengshuijiang city, Hunan province (P.R. China). Two contaminated profiles (CP = CP1+ CP2, 27°46'40" N, 111°29'47 " E) were selected as duplicates, representing soil sample that close to mine smelter. One uncontaminated profile (UCP, 27°44'48" N, 111°34'3" E) was selected as a control, representing soil sample that far away from core contaminated fields (> 8 kilometers). Collection of soil samples were summarized in Figure S1. In each field, 20 samples were collected from surface soil (0 m) to deep soil (2 m) at an interval of 0.1 m with a shovel. 20 samples were further group into level 1 (0–0.5 m), level 2 (0.5–1 m), level 3 (1–1.5 m), and level 4 (1.5–2 m) for statistical analysis. A total of 60 samples were collected for downstream analysis, including geochemical measurement and 16S rRNA sequencing. To determine the characterizations of microbial functional genes in different profile depths, 14 out of 60 samples were sent for shotgun metagenome sequencing, including 6 samples from CP1 (represents level 1–4), 6 samples from CP2 (represents level 1–4), and 2 samples from UCP as a comparison.

Geochemical parameter measurement

Soil samples (*n* = 60) were freeze-dried (vacuum freeze dryer, Scientz, Ningbo, China) for 48 h. Leaves, plant roots, and gravel in the soils were removed through a 2–mm sieve. Soil samples were then further thoroughly ground by a mortar and pestle before passing a 200–mesh sieve. Ten grams of dry soils were mixed with 25 mL distilled water. The mixture was shaken for 5 min, and then stand for 20 min to equilibrate. The measurement of geochemical parameters including oxidation reduction potential (Eh), pH, nitrate concentration, sulfate concentration, total organic carbon (TOC), Fe(II) and Fe(III) concentration, as well as the total concentration of As (As_{tot}) and Sb (Sb_{tot}), and their easily exchangeable fraction (*-exe*, Sb_{exe} and As_{exe}) and specifically absorbed surface-bound fraction (*-srp*, Sb_{srp} and As_{srp}). Details can be found in the supplementary files, including sample preparation, extraction condition, and analytical equipment.

DNA extraction

Samples for microbial community analyses (*n* = 60) were sieved to 2 mm and frozen at −80 °C until soil DNA was extracted. Soil DNA was extracted from approximately 0.5 g of air-dry soil using a FastDNA spin kit for soil (MP Biomedicals, Cleveland, OH, USA) and followed the manufacturer's instructions. DNA extracts were checked for quality and quantity using a Nanodrop®ND-1000 UV-Vis Spectrophotometer (Nanodrop Technologies, Wilmington, USA)[13].

Illumina MiSeq sequencing of 16S rRNA amplicons

16S rRNA amplicon sequencing was carried out as described in our previous work [14]. In brief, DNA was PCR-amplified in triplicate using the 515F (5'-GTGYCAGCMGCCGCGGTAA-3') and 907R (5'-

CCYCAATTCMTTTRAGTTT-3') primers set to amplify the hypervariable region of the 16S rRNA gene [15]. Primers were tagged with unique barcodes for each sample. Supplementary file contains the detail information of PCR amplification. Amplicons were sent to Novogene for high-throughput sequencing (Novogene Bioinformatics Company, China, Illumina MiSeq platform). The 16S rRNA amplicon sequences were archived in the NCBI SRA database (No. PRJNA634794). The 16S rRNA gene sequence raw reads were merged, filtered, clustered into operational taxonomic units (OTUs, with a similarity of 97% as the threshold), then annotated against GreenGenes database following our established bioinformatic pipelines. Details for analytical pipelines can be found in the supplementary file.

Shotgun metagenomic sequencing

Genomic DNA of 14 soil samples were selected for the shotgun metagenomic sequencing (Figure S1) at the Illumina HiSeq-PE150 platform (Novogene Bioinformatics Company, China). Metagenomic libraries were prepared according to the instruction (www.mrdnalab.com). A total of 133 Gb raw data (averaged 9.5 GB per sample) was generated for bioinformatic analysis according to our established pipelines, including quality control, trimming, *do nove* assembling, gene quantification, and gene annotation [16, 17]. Details of bioinformatic pipelines and script arguments can be found in the supplementary file. Raw sequences of metagenome were deposited to NCBI with a project (No. PRJNA634794).

Statistical analyses

Statistical analyses of data, such as ANOVA test and regression fitting, were carried out using GraphPad Prism software (v. 8.0). Diversity and composition of microbial community were analyzed on the MicrobiomeAnalyst platform (http://www.microbiomeanalyst.ca/) [18]. STAMP software was used to perform the differential analysis [19]. The two-dimensional interaction (Spearman's correlation index) between the individual geochemical parameter and selected microbial taxa or gene was calculated in the R ('ggcorrplot' package). The connections were filtered to calculate the strong correlation ($|R| > 0.7$, $p < 0.05$). Co-occurrence network was constructed in Gephi software (v. 0.92) to present the pairwise interactions [20]. The topological properties of co-occurrence networks were also calculated in Gephi (e.g. degree and modularity). Random forest (RF) model, an advanced machine learning algorithm, was performed in R (v3.5, 'randomForest' package) to predict the variable importance of individual environmental factor on the alpha diversity of microbial community.

Results And Discussion

General characterization of soil profiles

In this study, contaminated soil profiles were sampled from two pollution conditions (i.e., CP1 and CP2 for more contaminated sites and UCP for an uncontaminated site). The experimental design and sample collection details are summarized in **Figure S1**. A statistical comparison of three profiles was conducted by a one-way ANOVA (**Figure 1A**). Overall, the contaminated sites (CP1 and CP2) were characterized by low pH, high Eh, and high concentrations of sulfate, ferrous (Fe(II)) iron, ferric (Fe(III)) iron, Sb_{tot}, and As_{tot}

($p < 0.01$). Additionally, CP1 and CP2 formed a similar cluster pattern of geochemical parameters and distinctly separated from UCP (**Figure 1B**). In the following analyses, CP1 and CP2 were grouped as "CP" due to their similar soil properties. At each level, CP demonstrated a significantly lower pH, but higher Eh and sulfate concentrations in all profile depths ($p < 0.0001$) (**Figure 2**). TOC contents and Fe_{tot} concentrations were significantly different in deep soils (1.5–2 m, $p < 0.001$) and surface (0–0.5 m, $p < 0.01$), respectively, while nitrate and Fe(II) concentrations were not significantly different at any depth.

The depth-resolved differences of Sb and As concentrations in each profile were also compared (**Figure 3**). In surface soil, CP was severely contaminated by smelting actives and the Sb_{tot} and As_{tot} concentrations were much higher than in UCP. The average values of Sb_{tot} concentration in CP was 10–20 fold higher than in UCP. The highest value of Sb_{tot} concentrations in CP was 815 mg/kg (0–0.5 m), which was much higher than the secondary standard of *Environmental Quality Standards for Soils in China* (10 mg/kg; GB15168-2008). The bioaccessible fractions (-*exe* and -*srp*) of Sb in surface soil of CP were also higher than UCP. Likewise, the highest As_{tot} concentration in CP was 70.8 mg/kg, which also exceeded the natural background values of agricultural land (1–40 mg/kg; GB15168-2018). The bioavailable fractions (-*exe* and -*srp*) of As in surface soil were not detectably different between UCP and CP.

As soil depths increased, Sb_{tot} and As_{tot} dramatically decreased to 141.9 and 38.1 mg/kg in deep soil (1.5–2 m), respectively. Similar descending trends from surface to deep soil were also detected in the -*exe* and -*srp* fractions of Sb and As. The concentrations of most Sb and As fractions significantly ($p < 0.01$) negatively correlated with the depths of the vertical profiles (except As_{srp}, which was not significant). Results suggested that Sb and As contamination mainly originated from smelting deposition in surface layer (< 0.5 m), with a downward migration in the vertical profiles (e.g., atmospheric deposition) [5]. Consequently, the effects of contamination gradually declined as soil depth increased. As expected, different contamination conditions at each soil depth had different effects on soil microorganisms.

Composition of microbial communities at different profile depths

The compositions of microbial communities were characterized by 16S rRNA amplicon sequencing. The Bray–Curtis-based principal coordinate analysis (PCoA) revealed that the distribution of microbial communities at each profile depth was strongly affected by Sb and As contamination in CP (**Figure S2**). Smelting contamination reduced the alpha diversity of microbial communities at each profile (**Figure 4A and B**). Random forest model suggested the low alpha diversity could be attributed to the contents of Sb_{tot} and As_{tot} (**Figure 4C**). The relative abundance of the top 10 phyla detected in the soil profiles are presented in **Figure S3**. The taxonomy analyses indicated that the soil microbiota in CP at different depths were dominated by Acidobacteria (18.8%–44.7%), Chloroflexi (8.7%–42.4%), and Proteobacteria (11.4%–27.1%). The distribution of these predominant phyla was not similar to those in UCP. Several phyla were more abundant in UCP that were not detected in CP throughout the soil profiles, including Planctomycetes, Bacteroidetes, Gemmatimonade, and Nitrospirae.

This study also characterized the depth-resolved microbial communities and found that many phyla exhibited different dynamics throughout soil depths (**Figure 5**). A previous study demonstrated that surface soil microbial communities are naturally distinct from deep soil communities in their composition and structure [21]. Consistently, the relative abundance of the predominant phyla in UCP, Acidobacteria, Actinobacteria, and Bacteroidetes, gradually decreased from surface soil (0–0.5 m) to deep soil (1.5–2 m), while the relative abundance of Gemmatimonadetes and Nitrospirae dramatically increased as soil depth increased. However, the depth-resolved microbial community compositions in CP were distinct compared to UCP. As soil depth increased, Chloroflexi and Thaumarchaeota were the most variable phyla. Their relative abundances gradually increased from surface to deep soil, ranging from 8.69% to 42.43% and 0.49% to 20.17%, respectively, but both phyla were found in low abundance in UCP at each depth. In contrast, the relative abundance of Acidobacteria and Proteobacteria in CP gradually decreased as soil depth increased. The distinct cluster pattern of the microbial communities (**Figure S2, S3**), as well as the highly variable abundance of microorganisms (**Figure 5**), indicated that the variation of Sb and As contamination along the vertical soil profiles shaped the predominant microbial communities and had a highly significant effect on the depth-resolved microbial communities in soils. The co-occurrence analysis supported this hypothesis (**Figure S4**). It was also observed that Sb_{tot} was one of the most important environmental drivers that affected soil microbiota due to its highly connected properties.

Microbial interaction networks at different profile depths

The above results provide important insight into how single members of soil microbial communities respond to soil properties. Therefore, the multitude of direct and indirect interactions that occur at the whole microbial community level were further investigated. Here, an applied co-occurrence network analysis uncovered a 16S rRNA gene data set containing > 4,800,000 sequences from all soil profile samples (n = 60) and calculated robust associations between microbial taxa. A total of eight co-occurrence networks were constructed (four CP networks and four UCP networks) to compare microbial interactions at different profile depths (**Figure 6A**). In UCP, the pattern of microbial interactions remained relatively stable from surface soil (0–0.5 m) to deep soil (1.5–2 m), as indicated by the connections between the nodes and edges. In contrast, the microbial interactions in CP showed an obvious changing pattern as soil depth increased. The potential interactions in deeper networks (less contaminated) were stronger than surface networks (heavily contaminated).

Results also revealed that there were remarkable differences in the topological parameters of the networks (**Figure 6B and 6C; Table S1**). The node number (representing keystone microbiomes) and cluster number (representing function modules of microbial communities) in CP were always lower than UCP, indicating weak interactions among soil microbiota in contaminated profiles. In particular, the node number in CP gradually increased from surface to deep soil, indicating that individual species became more connected with other patterns to perform syntrophic functions in deep soils than those in surface soil. Therefore, the cluster number of microbial communities gradually decreased and grouped into less modules. Additionally, the ratio of positive/negative edge numbers of each network was calculated (**Figure 6D and 6E; Table S1**). Both positive and negative edge number ratios in UCP were ~50%. As a

comparison, Sb and As contamination reduced the proportion of negative correlations in microbial co-occurrence networks, as the positive edge ratio was much higher than the negative edge in CP (70% vs. 30%). A previous modeling study suggested that communities with a large proportion of members connected through positive links were unstable. In such communities, its members may respond in tandem to environmental fluctuations, resulting in positive feedback and co-oscillation. In contrast, negative links may stabilize co-oscillation in these communities and promote network stability [22]. This theory is supported by the observations of this study, where the networks were loosely connected in heavily contaminated surface soil but gradually recovered and were well connected in the less contaminated deep soil.

A network analysis of the significant taxon co-occurrence patterns, beyond the basic inventory descriptions of the composition and diversity of the microbial communities, may help explore the structure of complex microbial communities across spatial and temporal gradients [23, 24]. We hypothesized that Sb and As concentrations, rather than soil resource availability, is the main factor responsible for the observed changes in microbial interactions throughout the vertical soil profiles. Previous studies demonstrated that Sb and As contamination had considerable effects on soil microbial community dynamics [1, 25, 26]. However, understanding how these complex microbial communities recover from disturbances in situ remains a major challenge. In this study, different components of the microbial communities responded differently to Sb and As contamination at different soil depths. As soil depth increased, Sb and As contamination significantly declined from surface to deep soil ($p < 0.0001$, **Figure 3**). Soil microbiota in CP were generally more resilient, but less resistant, than UCP. Thus, the potential interactions among soil microbiota gradually shifted from weak (in heavily contaminated surface soil) to strong (in less contaminated deep soil). This distinction between surface and deep soil can be associated with the direct or indirect effects of Sb and As contamination.

Sb and As contamination may influence C and N cycling

A total of 12 metagenomes from CP and 2 metagenomes from UCP were constructed to investigate microbial metabolic functions (**Figure S1**). Based on the shotgun metagenomic sequencing, further in-depth investigations of the fundamental biogeochemical processes uncovered how soil microbiota adapted to different levels of Sb and As contamination throughout soil profiles. Results revealed that microbial metabolic potential changed with soil depth. In the following sections, the genes involved in the C and N metabolism pathways were analyzed against the KEGG database.

C metabolism pathway: Generally, the relative abundances of the genes encoding the Arnon–Buchanan reductive citrate cycle (rTCA) pathway in both UCP and CP were much higher than the five carbon fixation pathways (**Figure 7A**). This observation may be attributed to the high energy efficiency of rTCA, as 2 ATP equivalents are required to form pyruvate, while > 5 ATP equivalents are required in other C fixation pathways, except the Wood–Ljungdahl pathway, which requires < 1 ATP equivalent [27, 28]. Additionally, most genes involved in C metabolism from CP samples were much lower than UCP throughout all soil profiles. Since C bioavailability is one of the most important determinants for microbial activity [29], the

low abundances of these genes indicated microbial growth at each depth was strongly restricted by smelting contamination.

Besides, several pathways in CP gradually increased from surface to deep top soil, including the rTCA, dicarboxylate-hydroxybutyrate cycle (DC/4-HB), and hydroxypropionate-hydroxybutylate cycle (3-HP/4-HB) pathways. However, a previous study reported that C metabolic potential and diversity decreased from surface to deep soil (negatively correlated with soil depth), as surface soil harbored a higher proportion of pre-adapted inhabitants for substrate metabolism [21]. Additionally, surface soils are rich in available C substrates due to the input of root exudates, surface litter, and root detritus. Because the quantity and quality of C substrates decline in deeper soil layers, the rates of C input at lower depths are generally low and C tends to be in limited availability [30].

Such discrimination may be explained by C cycling that was strongly inhibited by Sb and As contamination at each soil depth in CP, especially surface soil. As soil depth increased, Sb and As concentrations declined and the microbes involved in carbon cycling gradually recovered. These findings indicate that the effects of contamination were much greater than C availability in surface soil. This could be supported by the co-occurrence network analysis, where 4 major C metabolism pathways, rTCA, reductive pentose phosphate cycle (Calvin-Benson-Bassham cycle; CBB), 3-HP/4-HB, and DC/4-HB, were all negatively correlated with Sb_{tot} and As_{tot} concentrations (**Figure 7B**).

N metabolism pathway: Microbial-mediated N transformations are important for N cycling in the soil. Genes encoding the assimilatory nitrate reduction (nitrate → ammonia) and denitrification (nitrate → nitrogen) pathways were more abundant in CP samples (**Figure S5**). Although the relative abundances of most genes did not directly correlate with soil depths, nitric oxide reductase (*norB*) and nitrate/nitrite transporter (*narK*) positively correlated with As_{tot} or Sb_{tot}, suggesting that smelting contamination may promote the denitrification pathway. The enrichment of the assimilatory nitrate reduction and denitrification pathways reduce nitrate concentrations. During this process, nitrate serves as an electron acceptor and couples with As(III) for anaerobic oxidization [31]. These findings provide insight into microbial adaptation in As contaminated soils, as toxicity was largely reduced from As(III) to As(V). In contrast, genes encoding the nitrification (ammonia → nitrite) pathway were restricted by smelting contamination, as ammonia monooxygenase (*pmoABC*) was much lower in CP samples and gradually increased from surface (0–0.5 m) to deep soil (1.5–2 m).

Microbial resistance to Sb and As contamination

The depth-resolved microbial activity characterization indicated that innate microbiota was greatly affected by the contamination of Sb and As. Because As and Sb have similar chemical structures, microbes may use similar metabolic pathways to transform both As and Sb [1].

As resistance genes in UCP versus CP: Results revealed that genes related to the arsenic resistance transcriptional regulator (*arsR*) were more abundant than other genes (**Figure 8A**). A set of *ars* genes [encoding As(V) reduction] were enriched by contamination and widely detected in CP, including *arsR*,

arsB, *arsC*, *ACR3*, and *arsH*. These genes were previously found to be prevalent among sediment, activated sludge, and unpolluted soil [32, 33]. However, the genes encoding As(III) oxidation (i.e., *aoxAB*) were quite low in both UCP and CP. Genes encoding As(V) respiration reduction (*arr* genes) and As(III) methylation (*arsM*) were undetectable. The prevalence of *ars* genes could be ascribed to the versatility of As(V) reducing bacteria [34]. For example, one study found a broad phylogenetic distribution of *arsC* genes in soil bacteria, including *Rhizobiales*, *Burkholerials*, and *Geobacillus* [32]. In addition to *ars* genes, the relative abundance of arsenite-transporting ATPase (*ASNA1*) and arsenite transporter, the ACR3 family (*ACR3*) also increased in CP. Four gene types were solely detected in CP samples, including arsenical resistance protein (*arsH*), arsenical-resistance protein 2 (*ACR2*), arsenite methyltransferase (*AS3MT*), and arsenate-mycothiol transferase (*arsC*) (**Figure 8B**). The relatively high abundances of these genes in CP suggest that bacterial resistance in response to Sb and As contamination was enhanced [35], including the ability to confer resistance to arsenate and arsenite via operons (e.g., *arsR*, *arsB*, *arsC*) (Ji and Silver, 1992).

As resistance genes at different profile depths: The distributions of these As metabolism genes were highly variable throughout soil profiles in CP. The abundance of these genes decreased with soil depth (e.g., *arsB*, *ACR3*, and *arsC,* **Figure 8A and B**). The enrichment of these genes in surface soil may be attributed to the higher concentrations of As and Sb in top soil layers. Elevated As and Sb concentrations exerted strong natural selection on the present microbiota and, in turn, these microbiotas expressed more functional genes that encode the As detoxification process to relieve such perturbations. In contrast, several other genes increased with soil depth (e.g., *arsR*). The detection of highly abundant As resistance genes in deep soil layers implied that Sb and As contamination affected the whole soil profile, even at a depth of 2 m. Thus, these findings indicate that Sb and As pollution treatments should not be limited to surface soil remediation and that the distribution, migration, and toxicity of Sb and As pollution in deep layers should also be considered.

Correlation of As resistance genes and contaminations: In addition to the highly variable abundances of As-related genes in CP, strong correlations were detected among these genes and concentrations of As fractions (**Figure 8C**), such as *ACR3* and *arsB*. A previous study detected a positive correlation between the total abundances of As-related genes and As_{tot} concentrations [36]. A separate study found that the abundances of genes involved in different As biotransformation processes also positively correlated with different As species in soil samples [37]. Furthermore, in this study, strong correlations of these As-related genes and Sb fractions were observed. For example, Sb_{tot} positively correlated with *arsB* and *ACR3*, suggesting the potential roles of these genes in Sb metabolism and contamination may promote the proliferation of such genes. Because As and Sb share structural similarities, microorganisms may use similar metabolic pathways to transform both As and Sb. A previous study reported that As and Sb induced arsenic-resistant operons, which contain an arsenical pump membrane protein (*arsB*) [38]. Similarly, YL Meng, Z Liu and BP Rosen [39] reported that the ArsB family can catalyze the transport of Sb fractions. Genomic sequencing of *Comamonas* sp. S44 (an Sb-oxidizing bacterium) revealed the presence of genes encoding ArsB [40]. Therefore, it is proposed that Sb redox may be catalyzed by

enzymes that are encoded by the same As-related functional genes. However, due to the limited database of genes encoding Sb cycling and resistance in KEGG functional categories, this hypothesis requires further investigation based on cultured isolations of Sb-metabolizing bacteria.

Conclusions

This study compared soil profiles (0–2 m) with and without Sb and As contamination that directly originated from smelting activities. Heavy Sb and As contamination significantly lowered the soil pH and increased the Eh and sulfate concentrations throughout the soil profiles. Sb and As concentrations accumulated in surface soil, but declined with soil depth. The gradually changing Sb and As contents greatly changed the relative abundance of soil microbiota as soil depth increased, including Acidobacteria, Proteobacteria, Chloroflexi, and Thaumarchaeota. Microbial interaction networks were loosely connected in surface soil but gradually recovered in deep soil, suggesting that individual species became more connected with other patterns to perform syntrophic functions in the less contaminated soil depth. The metagenomic results indicated that microbial metabolic traits also changed in response to different levels of Sb and As contamination throughout the soil profiles, including promoting the abundance of several genes encoding As resistance or restricting genes that encode C metabolism pathways.

Declarations

Conflict of Interest

The authors declare that they have no conflict of interest.

Acknowledgements

We thank LetPub (www.letpub.com) for its linguistic assistance during the preparation of this manuscript.

Authors’ contributions

RX and WS designed research. XS, FH, EX, LQ, and ZY performed the research. RX, BL, and BS analyzed data. RX and WS wrote the paper. All authors read and approved the final manuscript.

Funding

This work was supported by China Postdoctoral Science Foundation funded Project (Grant No. 2019M662825), Guangdong Basic and Applied Basic Research Foundation (Grant No. 2019A1515110351), the Science and Technology Planning Project of Guangzhou (Grant Nos. 202002030271 and 202002020072), GDAS' Project of Science and Technology Development (Grant Nos. 2020GDASYL-20200103086, 2019GDASYL-0103046, 2019GDASYL-0103052 and 2019GDASYL-0301002) the Local Innovative and Research Teams Project of Guangdong Pearl River Talents Program

(Grant No. 2017BT01Z176), Guangdong Foundation for Program of Science and Technology Research (Grant No. 2019B121205006), and Guangdong Introducing Innovative and Entrepreneurial Talents (Grant No. 2017GC010570).

Availability of data and materials

The obtained sequences were submitted to the NCBI Sequence Read Archive (SRA) with accession number No. PRJNA634794 (https://www.ncbi.nlm.nih.gov/sra/uploads/tech@ecogene-biotech.com_N0QEqK0Q/PRJNA634794). Other data and result supporting the findings of the study are available in this article and its supplementary information files.

Ethics approval and consent to participate

Not applicable.

Consent for publication

Not applicable.

Competing interests

The authors declare that they have no competing interests.

References

1. Sun W, Xiao E, Xiao T, Krumins V, Wang Q, Häggblom M, Dong Y, Tang S, Hu M, Li B *et al*: Response of Soil Microbial Communities to Elevated Antimony and Arsenic Contamination Indicates the Relationship between the Innate Microbiota and Contaminant Fractions. *Environ Sci Technol* 2017, 51(16):9165-9175.
2. Hans Wedepohl K: The composition of the continental crust. *Geochim Cosmochim Acta* 1995, 59(7):1217-1232.
3. Filella M, Belzile N, Chen Y-W: Antimony in the environment: a review focused on natural waters: I. Occurrence. *Earth-Sci Rev* 2002, 57(1):125-176.
4. Ye L, Qiu S, Li X, Jiang Y, Jing C: Antimony exposure and speciation in human biomarkers near an active mining area in Hunan, China. *Sci Total Environ* 2018, 640-641:1-8.
5. Xiao E, Krumins V, Xiao T, Dong Y, Tang S, Ning Z, Huang Z, Sun W: Depth-resolved microbial community analyses in two contrasting soil cores contaminated by antimony and arsenic. *Environ Pollut* 2017, 221:244-255.
6. Wilson SC, Lockwood PV, Ashley PM, Tighe M: The chemistry and behaviour of antimony in the soil environment with comparisons to arsenic: A critical review. *Environ Pollut* 2010, 158(5):1169-1181.
7. Li J, Wang Q, Oremland RS, Kulp TR, Rensing C, Wang G: Microbial Antimony Biogeochemistry: Enzymes, Regulation, and Related Metabolic Pathways. *Appl Environ Microbiol* 2016, 82(18):5482-

5495.

8. Li J, Zheng B, He Y, Zhou Y, Chen X, Ruan S, Yang Y, Dai C, Tang L: Antimony contamination, consequences and removal techniques: a review. *Ecotoxicol Environ Saf* 2018, 156:125-134.
9. Sun W, Xiao E, Xiao T, Krumins V, Wang Q, Haggblom M, Dong Y, Tang S, Hu M: Response of soil microbial communities to elevated antimony and arsenic contamination indicates the relationship between the innate microbiota and contaminant fractions. *Environ Sci Technol* 2017, 51(16):9165.
10. Li C, Yan K, Tang L, Jia Z, Li Y: Change in deep soil microbial communities due to long-term fertilization. *Soil Biol Biochem* 2014, 75:264-272.
11. Filella M: Antimony interactions with heterogeneous complexants in waters, sediments and soils: A review of data obtained in bulk samples. *Earth-Sci Rev* 2011, 107(3):325-341.
12. Blume E, Bischoff M, Reichert JM, Moorman T, Konopka A, Turco RF: Surface and subsurface microbial biomass, community structure and metabolic activity as a function of soil depth and season. *Applied Soil Ecology* 2002, 20(3):171-181.
13. Xu R, Yang Z, Zheng Y, Zhang H, Liu J, Xiong W, Zhang Y, Ahmad K: Depth-resolved microbial community analyses in the anaerobic co-digester of dewatered sewage sludge with food waste. *Bioresour Technol* 2017, 244:824-835.
14. Xu R, Sun X, Han F, Li B, Xiao E, Xiao T, Yang Z, Sun W: Impacts of antimony and arsenic co-contamination on the river sedimentary microbial community in an antimony-contaminated river. *Sci Total Environ* 2020, 713:136451.
15. Kuczynski J, Stombaugh J, Walters WA, Gonzalez A, Caporaso JG, Knight R: Using QIIME to analyze 16S rRNA gene sequences from microbial communities. *Current protocols in bioinformatics* 2011, Chapter 10:Unit 10.17.
16. Sun X, Kong T, Häggblom MM, Kolton M, Li F, Dong Y, Huang Y, Li B, Sun W: Chemolithoautotropic Diazotrophy Dominates the Nitrogen Fixation Process in Mine Tailings. *Environ Sci Technol* 2020, 54(10):6082-6093.
17. Xu R, Yang Z, Zheng Y, Wang Q, Bai Y, Liu J, Zhang Y, Xiong W, Lu Y, Fan C: Metagenomic analysis reveals the effects of long-term antibiotic pressure on sludge anaerobic digestion and antimicrobial resistance risk. *Bioresour Technol* 2019, 282:179-188.
18. Dhariwal A, Chong J, Habib S, King IL, Agellon LB, Xia J: MicrobiomeAnalyst: a web-based tool for comprehensive statistical, visual and meta-analysis of microbiome data. *Nucleic Acids Res* 2017, 45(W1):W180-W188.
19. Parks DH, Tyson GW, Hugenholtz P, Beiko RG: STAMP: statistical analysis of taxonomic and functional profiles. *Bioinformatics* 2014, 30(21):3123-3124.
20. Xu R, Yang Z, Zheng Y, Liu J, Xiong W, Zhang Y, Lu Y, Xue W, Fan C: Organic loading rate and hydraulic retention time shape distinct ecological networks of anaerobic digestion related microbiome. *Bioresour Technol* 2018, 262:184-193.
21. Fierer N, Schimel JP, Holden PA: Variations in microbial community composition through two soil depth profiles. *Soil Biol Biochem* 2003, 35(1):167-176.

22. Coyte KZ, Schluter J, Foster KR: The ecology of the microbiome: Networks, competition, and stability. *Science (New York, NY)* 2015, 350(6261):663.
23. Barberán A, Bates ST, Casamayor EO, Fierer N: Using network analysis to explore co-occurrence patterns in soil microbial communities. *The ISME journal* 2012, 6(2):343-351.
24. Xu R, Li B, Xiao E, Young LY, Sun X, Kong T, Dong Y, Wang Q, Yang Z, Chen L *et al*: Uncovering microbial responses to sharp geochemical gradients in a terrace contaminated by acid mine drainage. *Environ Pollut* 2020, 261:114226.
25. Singh R, Singh S, Parihar P, Singh VP, Prasad SM: Arsenic contamination, consequences and remediation techniques: A review. *Ecotoxicol Environ Saf* 2015, 112:247-270.
26. Filella M, Williams PA, Belzile N: Antimony in the environment: knowns and unknowns. *Environmental Chemistry* 2009, 6(2):95-105.
27. Bar-Even A, Noor E, Milo R: A survey of carbon fixation pathways through a quantitative lens. *J Exp Bot* 2011, 63(6):2325-2342.
28. Sun W, Sun X, Li B, Xu R, Young LY, Dong Y, Zhang M, Kong T, Xiao E, Wang Q: Bacterial response to sharp geochemical gradients caused by acid mine drainage intrusion in a terrace: Relevance of C, N, and S cycling and metal resistance. *Environ Int* 2020, 138:105601.
29. Wardle D: A comparative assessment of factors which influence microbial biomass carbon and nitrogen levels in soil. *Biological reviews* 1992, 67(3):321-358.
30. Richter DD, Markewitz D: How Deep Is Soil? *Bioscience* 1995, 45(9):600-609.
31. Oremland RS, Stolz JF: The ecology of arsenic. *Science (New York, NY)* 2003, 300(5621):939-944.
32. Xiao K-Q, Li L-G, Ma L-P, Zhang S-Y, Bao P, Zhang T, Zhu Y-G: Metagenomic analysis revealed highly diverse microbial arsenic metabolism genes in paddy soils with low-arsenic contents. *Environ Pollut* 2016, 211:1-8.
33. Cai L, Yu K, Yang Y, Chen B-w, Li X-d, Zhang T: Metagenomic exploration reveals high levels of microbial arsenic metabolism genes in activated sludge and coastal sediments. *Appl Microbiol Biotechnol* 2013, 97(21):9579-9588.
34. Silver S, Phung LT: Genes and enzymes involved in bacterial oxidation and reduction of inorganic arsenic. *Appl Environ Microbiol* 2005, 71(2):599-608.
35. Rosenstein R, Peschel A, Wieland B, Götz F: Expression and regulation of the antimonite, arsenite, and arsenate resistance operon of Staphylococcus xylosus plasmid pSX267. *J Bacteriol* 1992, 174(11):3676-3683.
36. Zhang S-Y, Zhao F-J, Sun G-X, Su J-Q, Yang X-R, Li H, Zhu Y-G: Diversity and abundance of arsenic biotransformation genes in paddy soils from southern China. *Environ Sci Technol* 2015, 49(7):4138-4146.
37. Jia Y, Huang H, Chen Z, Zhu Y-G: Arsenic uptake by rice is influenced by microbe-mediated arsenic redox changes in the rhizosphere. *Environ Sci Technol* 2014, 48(2):1001-1007.

38. Ji G, Silver S: Reduction of arsenate to arsenite by the ArsC protein of the arsenic resistance operon of Staphylococcus aureus plasmid pI258. *Proceedings of the National Academy of Sciences of the United States of America* 1992, 89(20):9474-9478.
39. Meng YL, Liu Z, Rosen BP: As(III) and Sb(III) uptake by GlpF and efflux by ArsB in Escherichia coli. *J Biol Chem* 2004, 279(18):18334-18341.
40. Li J, Wang Q, Zhang S, Qin D, Wang G: Phylogenetic and genome analyses of antimony-oxidizing bacteria isolated from antimony mined soil. *Int Biodeterior Biodegrad* 2013, 76:76-80.

Figures

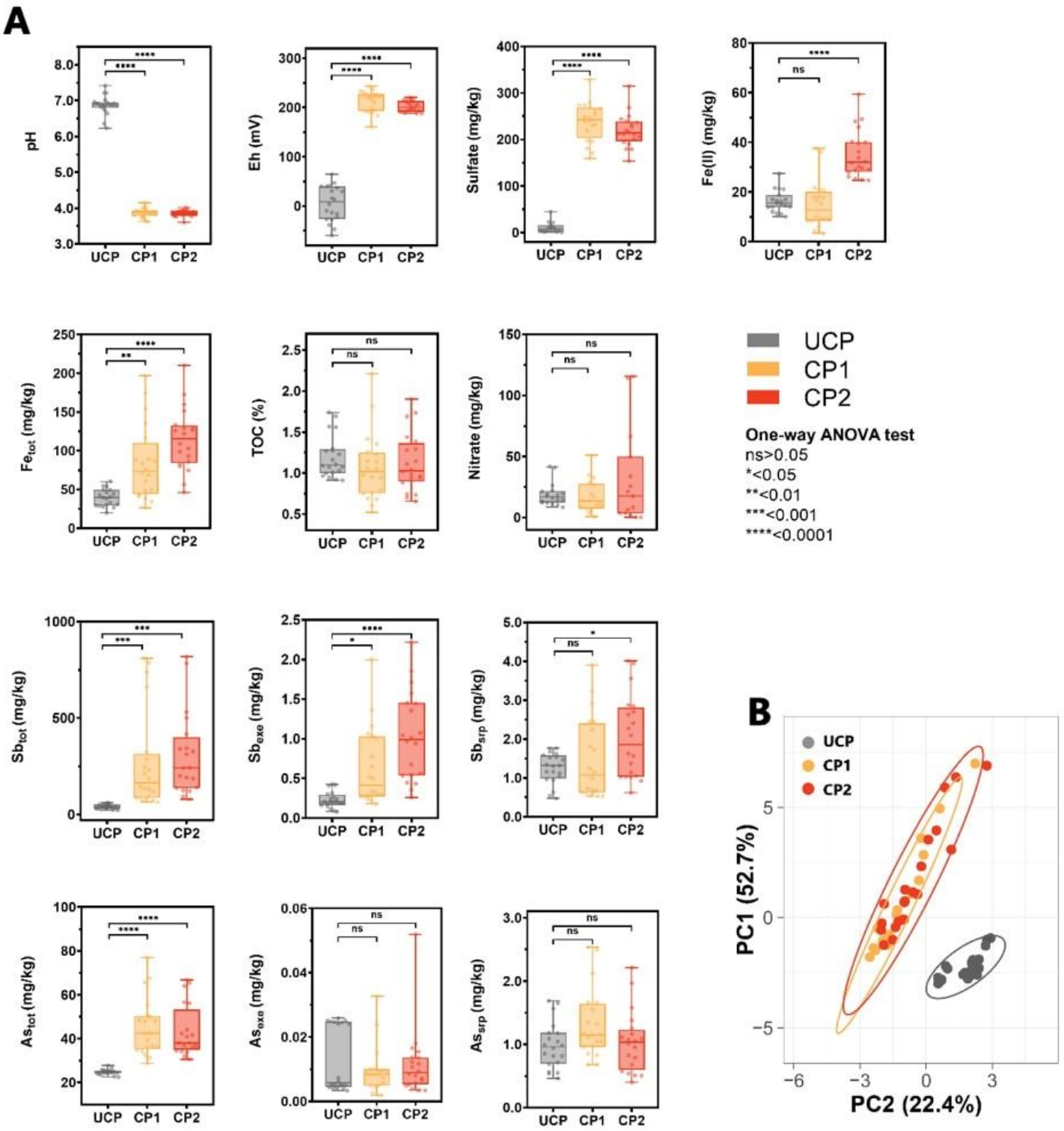

Figure 1

. (A) Comparison of geochemical parameters in one uncontaminated profile (UCP) and two contaminated profiles (CP1, CP2, as duplicates). The difference among three profiles were exammed by one-way ANOVA test. The asterisk sign represents the statistical significance (for p: *<0.05, **<0.01, ***<0.001, **** <0.0001, ns for Not Significant). (B) Principal component analysis (PCA) indicated the CP1 and CP2

samples highly overlapped but distinctly separated from UCP samples, based on the geochemical parameters.

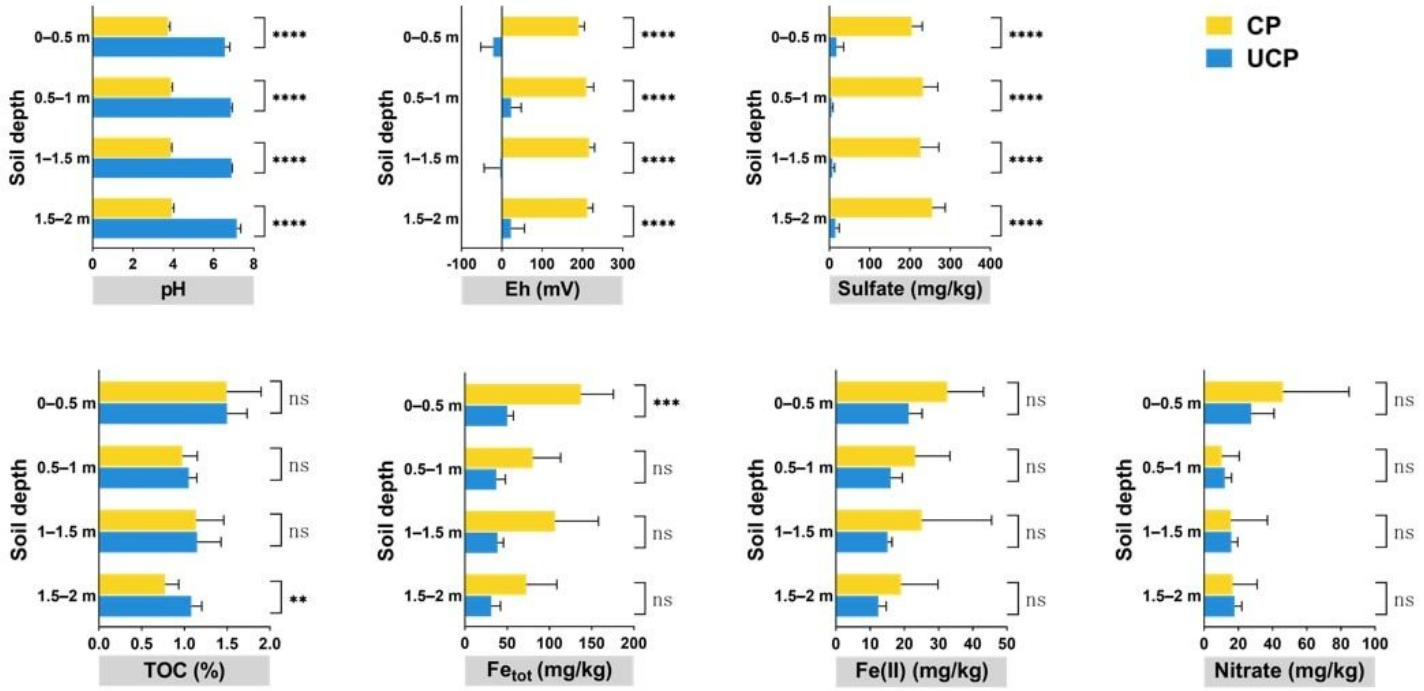

Figure 2

Changes in various geochemical parameters at different soil depths (0–2 m) in two contaminated profiles (CP = CP1 + CP2) and one uncontaminated profile (UCP). Error bars represent the standard error of the mean. The difference between UCP and CP at each level were exammed by multiple t-test. The asterisk sign represents the statistical significance (*p < 0.05, **p < 0.01, ***p < 0.001, ****p < 0.0001, ns: Not Significant).

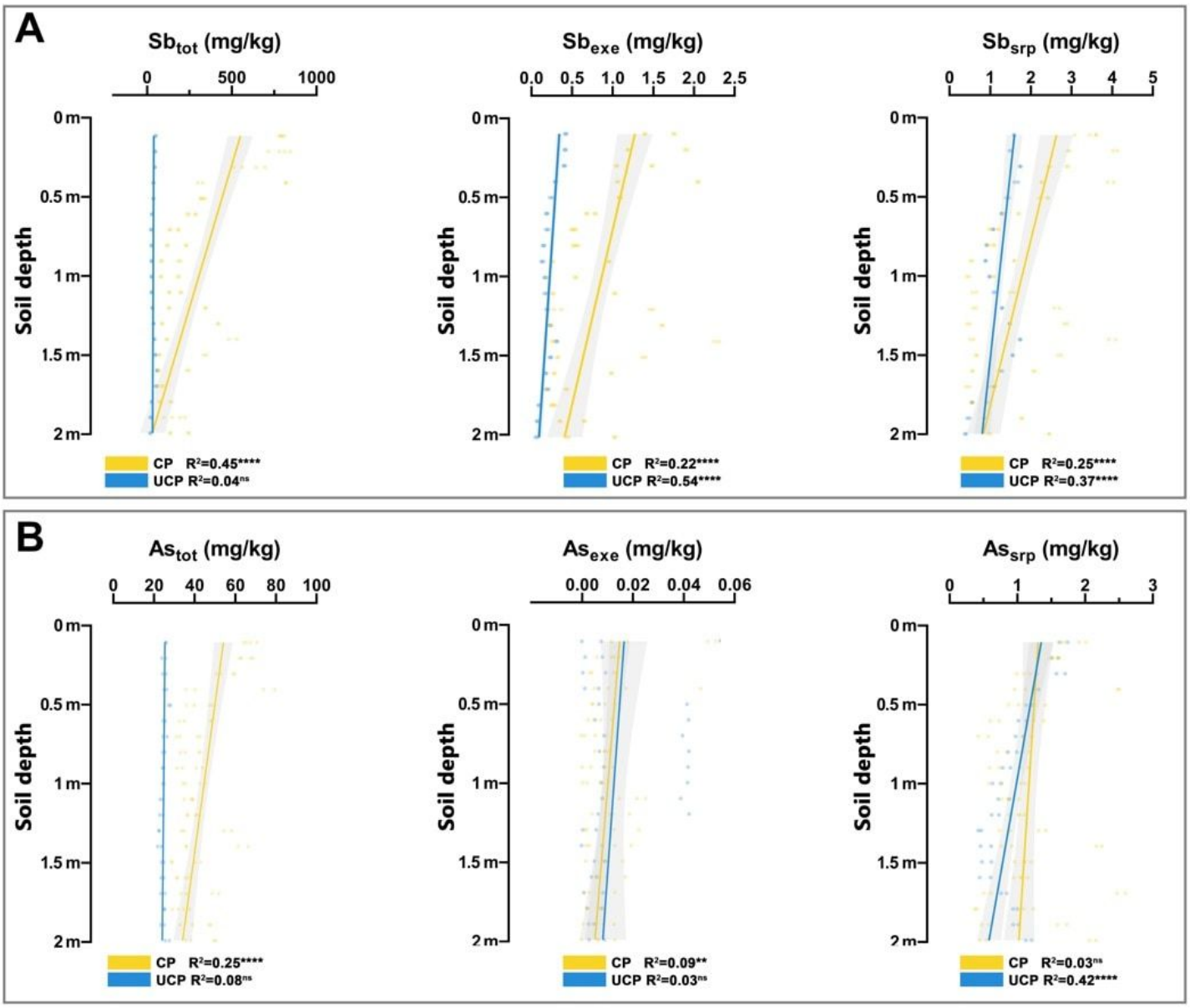

Figure 3

Distribution of Sb (A) and As concentrations (B) in the vertical soil profiles (UCP versus CP). Each point represents an individual sample. Solid lines represent the linear regression modules. The grey area represents the 95% confidence interval. The asterisk sign represents the statistical significance of linear regression modules (**p < 0.01, **** p < 0.0001, ns: Not Significant).

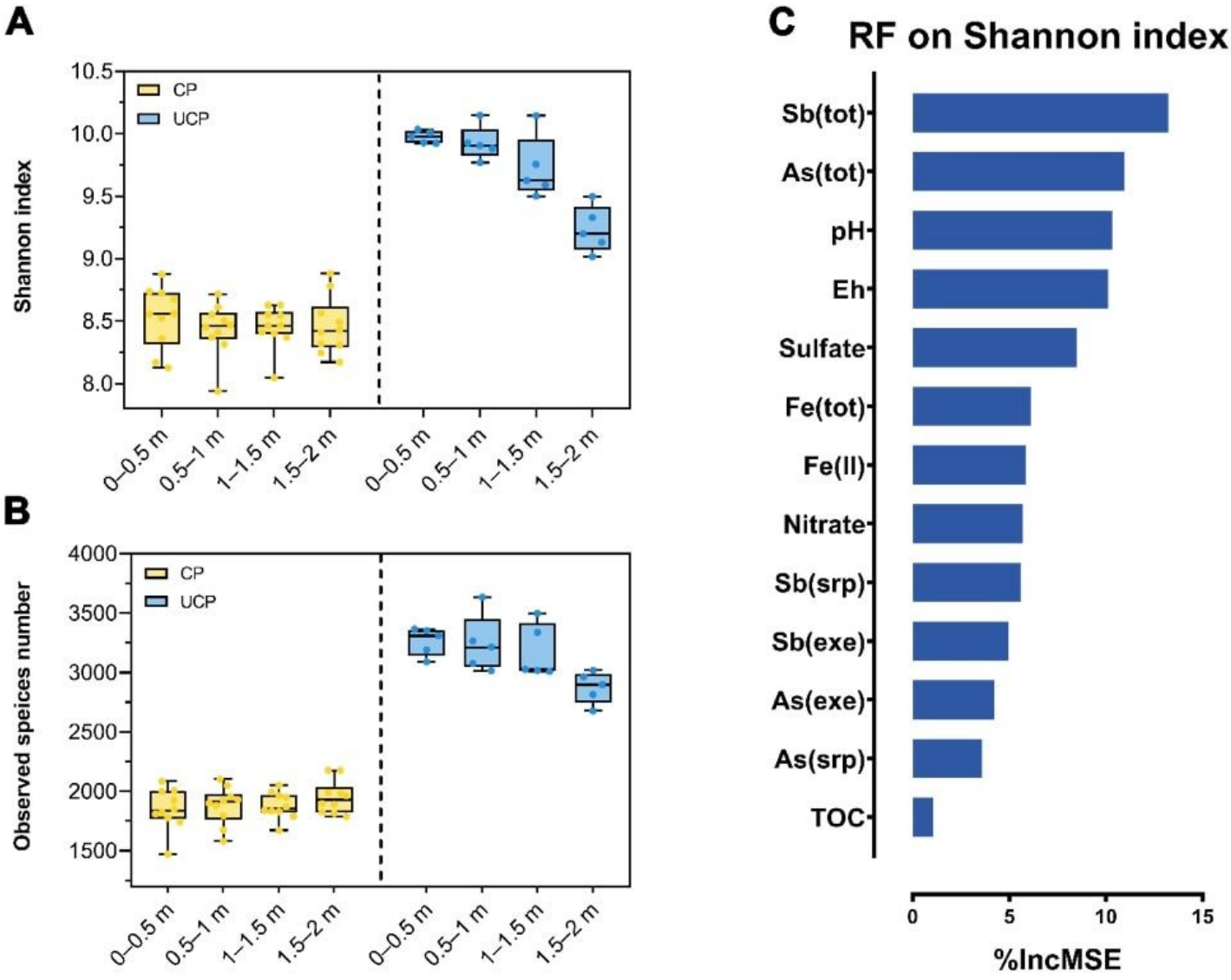

Figure 4

Alpha diversity index at different depths in two contaminated profiles (CP = CP1 + CP2) and one uncontaminated profile (UCP), as revealed by the (A) Shannon index and (B) observed species number. (C) The random forest (RF) model predicted the effects of various geochemical parameters on Shannon index. Variables with a large mean decrease in accuracy (%IncMSE) are more important for classification of the data.

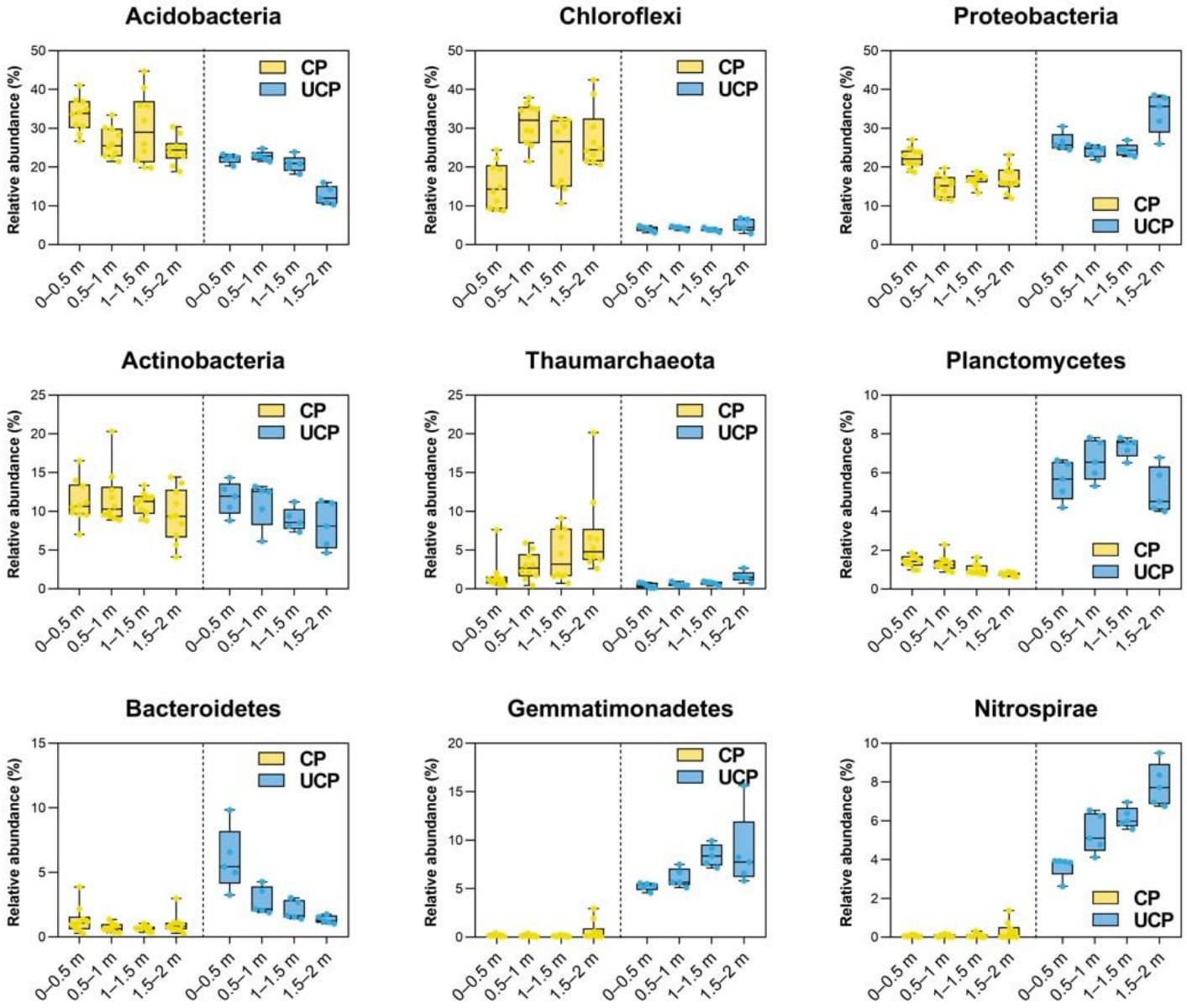

Figure 5

Microbial community compositions of two contaminated profiles (CP = CP1+CP2) and one uncontaminated profile (UCP). The box charts indicate the dynamic changes of the relative abundances of the top 10 phyla from surface (0–0.5 m) to deep soil (1.5–2 m).

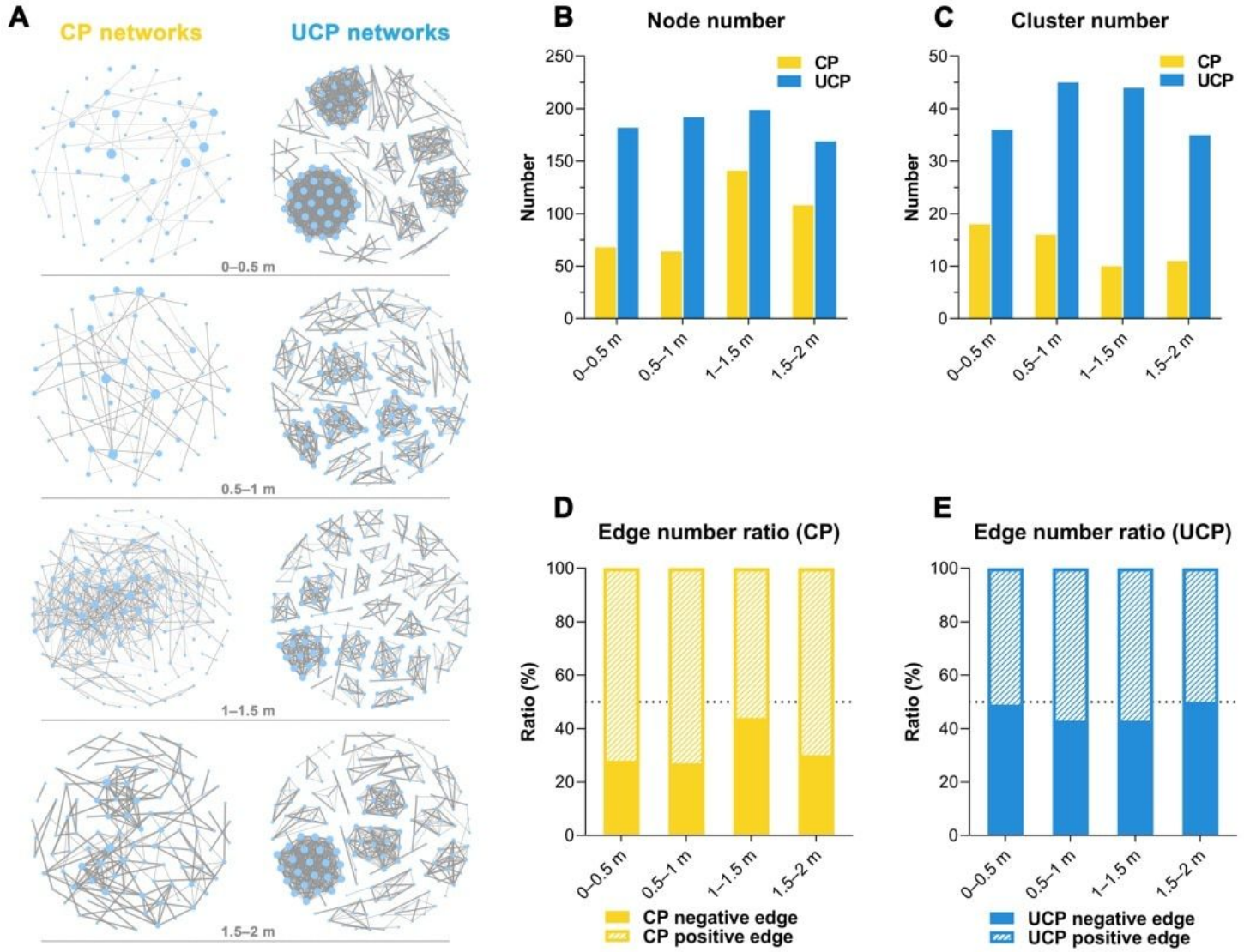

Figure 6

Microbial interactions at different depths in one uncontaminated profile (UCP) and two contaminated profiles (CP = CP1 + CP2), as revealed by the patterns of co-occurrence networks (A). A connection (node-edge-node) indicates a strong (Spearman's |R| > 0.7) and significant ($p < 0.01$) correlation between two OTUs. The topological characterizations of eight networks are also provided, including (B) node number, (C) cluster number, (D) edge number ratio (positive edge versus negative edge) in UCP, and (E) edge number ratio in CP.

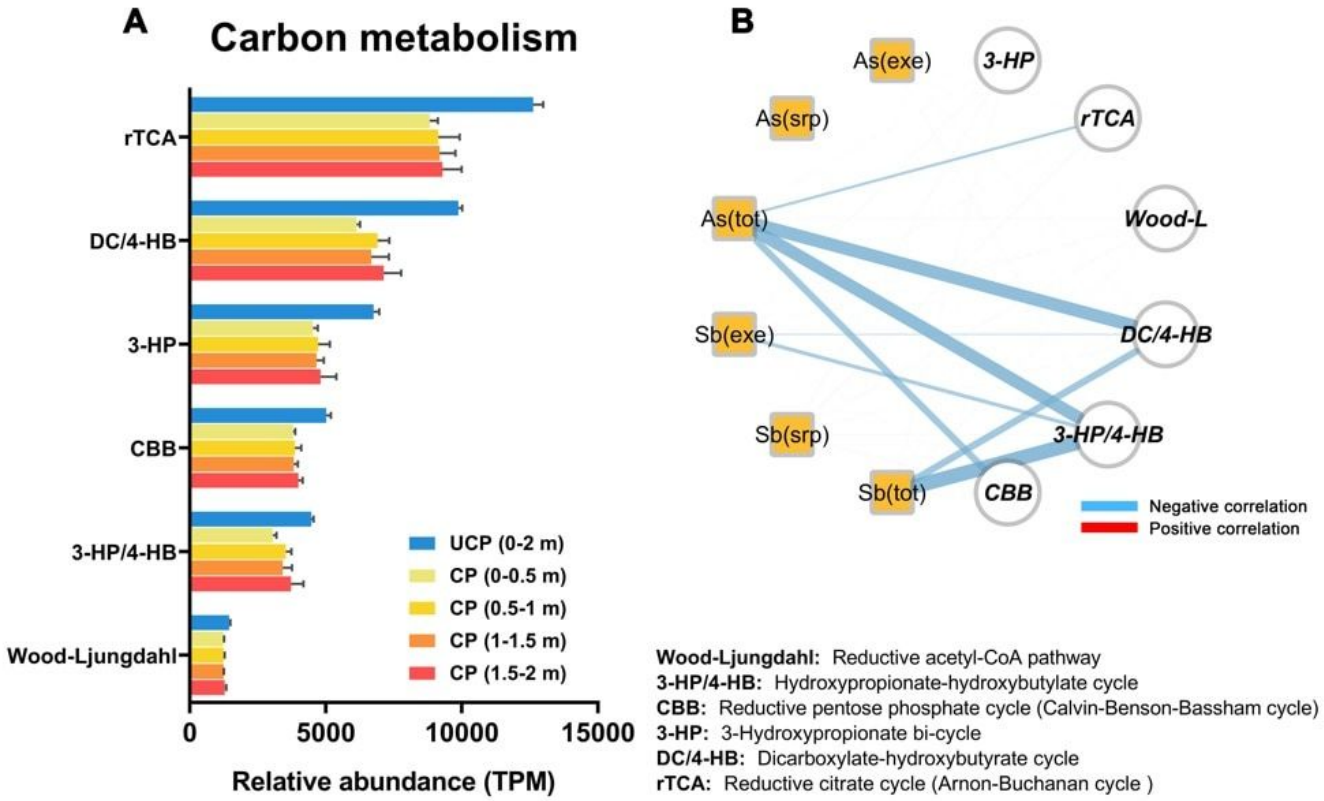

Figure 7

Detection of genes encoding C metabolism pathways. (A) General distribution of detected genes. (B) Correlation of pathways abundance and geochemical parameters. Red and blue lines indicate the positive and negative Spearman's correlations ($|R| > 0.7$, $p < 0.05$), respectively. Edge width is proportional to the correlation value.

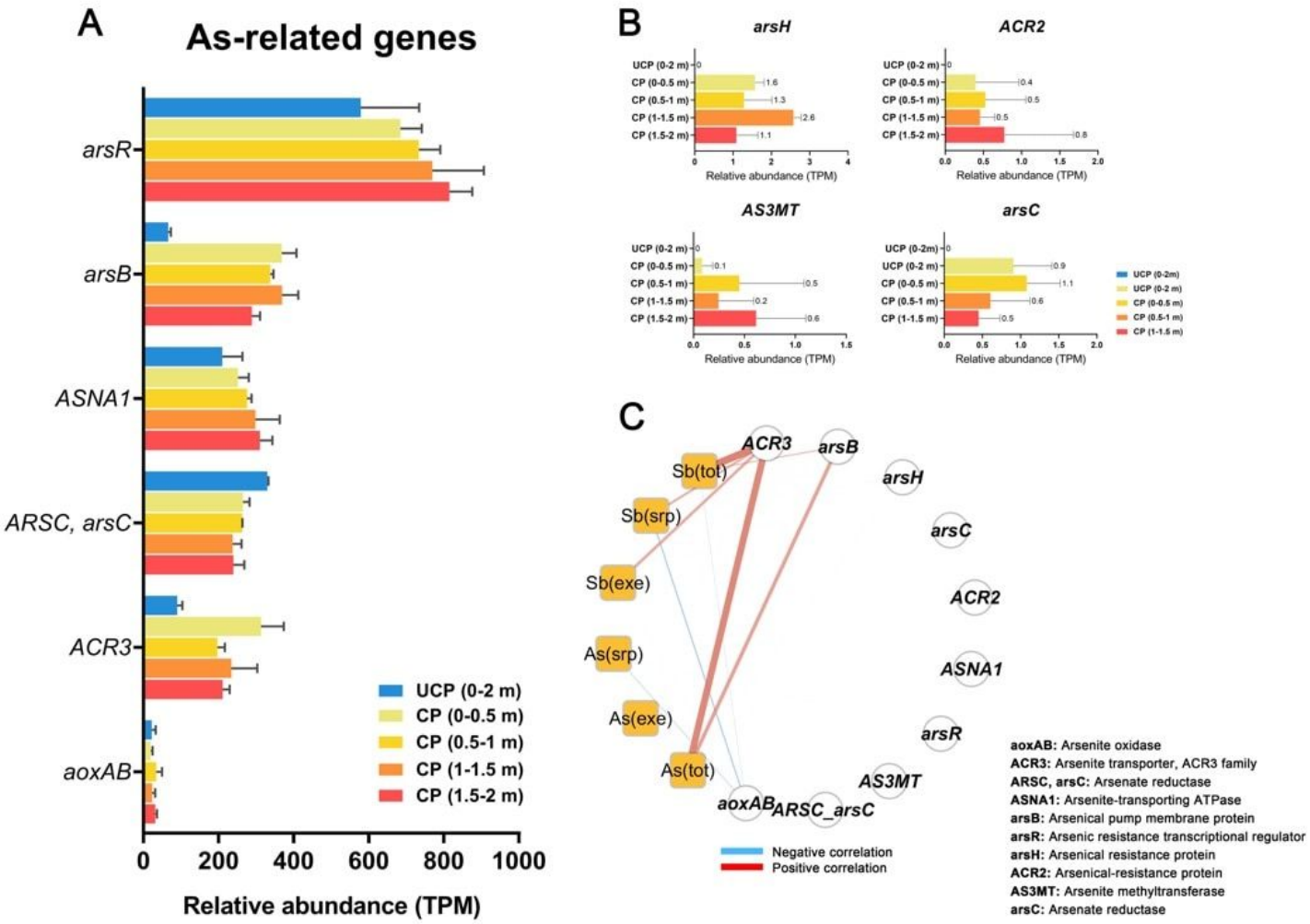

Figure 8

Detection of arsenic-related genes in UCP and CP samples by shotgun metagenomic sequencing. (A) General distribution of detected genes. (B) Genes solely detected in CP profiles. (C) Correlation of detected genes abundance and geochemical parameters. Red and blue lines indicate the positive and negative Spearman's correlations ($|R| > 0.7$, $p < 0.05$), respectively. Edge width is proportional to the correlation value.

Supplementary Files

This is a list of supplementary files associated with this preprint. Click to download.

- 6.Supportinginformation.docx